Journal of Zhejiang University-SCIENCE A (Applied Physics & Engineering)
ISSN 1673-565X (Print); ISSN 1862-1775 (Online)
www.zju.edu.cn/jzus; www.springerlink.com
E-mail: jzus@zju.edu.cn

Buckling of thin-walled beams by a refined theory

Syed Muhammad IBRAHIM†1, Erasmo CARRERA†‡2, Marco PETROLO[2], Enrico ZAPPINO[2]

([1]*Specialty Units for Safety and Preservation of Structures, King Saud University, Riyadh, Saudi Arabia*)

([2]*Department of Mechanical and Aerospace Engineering, Politecnico di Torino, Corso Duca degli Abruzzi 24, 10129 Torino, Italy*)

†E-mail: {muhammad.syed; erasmo.carrera}@polito.it

Received Dec. 8, 2011; Revision accepted Apr. 1, 2012; Crosschecked Sept. 24, 2012

Abstract: The buckling of thin-walled structures is presented using the 1D finite element based refined beam theory formulation that permits us to obtain N-order expansions for the three displacement fields over the section domain. These higher-order models are obtained in the framework of the Carrera unified formulation (CUF). CUF is a hierarchical formulation in which the refined models are obtained with no need for ad hoc formulations. Beam theories are obtained on the basis of Taylor-type and Lagrange polynomial expansions. Assessments of these theories have been carried out by their applications to studies related to the buckling of various beam structures, like the beams with square cross section, I-section, thin rectangular cross section, and annular beams. The results obtained match very well with those from commercial finite element softwares with a significantly less computational cost. Further, various types of modes like the bending modes, axial modes, torsional modes, and circumferential shell-type modes are observed.

Key words: Unified beam theory, Carrera unified formulation (CUF), Buckling, 1D formulation
doi:10.1631/jzus.A1100331 **Document code:** A **CLC number:** TU2

1 Introduction

Beam theories are extensively used to analyze the structural behavior of slender bodies, such as the ones used in civil, aeronautical as well as mechanical engineering applications. 1D structural models are simpler and computationally cheaper than 2D (plate/shell) and 3D (solid) elements. Further, beams can also be the representatives of 2D structures undergoing cylindrical bending. This aspect makes beam theories attractive for the static and dynamic analyses of structures.

Accurate analysis using the refined theories, incorporating the non-classical effects which can not be obtained with the Euler-Bernoulli beam theory (EBBT) and Timoshenko beam theory (TBT) (EBBT does not account for transverse shear deformations and TBT considers a uniform shear distribution along the cross section of a beam), is of paramount importance for thin-walled composite structures frequently used in modern engineering applications, like aerospace, marine and civil structural components, wherein weight to strength ratio is given due importance.

A first attempt to improve beams models is related to the use of shear correction factors, as clearly stated in Sokolnikoff (1956), Novozhilov (1961), and Timoshenko and Woinowski-Krieger (1970). Many works have been presented on this topic, for example, Cowper (1966), Gruttmann *et al.* (1999), Gruttmann and Wagner (2001), and Wagner and Gruttmann (2002) for static analysis; Stephen (1980) and Hutchinson (2001) for dynamics. Moreover, Jensen (1983) showed how the shear correction factor varies with the natural frequencies. However, as shown first in the reviews by Kaneko (1975) and recently by Dong *et al.* (2010), the definition of a universally accepted formulation for shear correction factors is not an easy task.

‡ Corresponding author

Ladevèze and Simmonds (1996; 1998), El Fatmi (2002; 2007a; 2007b), and Ladevèze *et al.* (2004) introduced improvements of the displacement models over the beam section by introducing warping functions. Further, beam theories were based on the displacements field proposed by Ieşan (1986) and were solved by a semi-analytical finite element method (FEM) by Dong *et al.* (2001), Kosmatka *et al.* (2001), and Lin and Dong (2006). Rand (1994) and Kim and White (1997) used the same approach in the free vibration analysis introducing out-of-plane warping with no in-plane stretching terms.

Asymptotic type expansions in conjunction with variational methods have been proposed by Berdichevsky *et al.* (1992) which includes a commendable review of prior works on the beam theory development. It is the origin of an alternative approach to constructing refined beam theories. Some further valuable contributions are those by Volovoi *et al.* (1999), Popescu and Hodges (2000), Yu *et al.* (2002), and Yu and Hodges (2004; 2005). A dynamic extension has been proposed by Kim and Wang (2010) and by Firouz-Abadi *et al.* (2007) where the Wentzel-Kramers-Brillouin (WKB) approximation was used.

The generalized beam theory (GBT) was originated with Schardt's works (Schardt, 1966; 1994; Schardt and Heinz, 1991). GBT improves classical theories by using piece-wise beam description of thin-walled sections. It has been widely employed and extended in various forms by Silvestre (2002; 2007) and Silvestre and Camotim (2002), and a dynamic application is presented by Bebiano *et al.* (2008).

A hierarchical approach with variable kinematic 2D models has been successfully developed by Carrera (1995; 2003) and Carrera and Demasi (2002). Carrera unified formulation (CUF) is a hierarchical formulation which permits a systematic evaluation of refined higher-order plate models from classic 2D models to quasi-3D descriptions for both static and dynamic analyses—without the need for ad hoc assumptions (Carrera, 1995; 2000; Carrera and Giunta, 2009). It can be noted that the evaluation of the 2D approximations against the buckling of composite plates and shell models was recently proposed in D'Ottavio and Carrera (2010) and Nali *et al.* (2011), which are carried out within the framework of CUF. However, the 2D models used for structures are complex and computational expensive, thereby a need for a much simpler model was brought out.

Recently, Demasi (2009) presented the generalized unified formulation (GUF) approach. This method is an extension of CUF used in this work. The GUF introduces a new formulation that allows to derive the FEM matrix using a 1×1 fundamental nucleus.

Some studies using the hierarchical beam theories embedded in the CUF have also been carried out. Carrera and Giunta (2010) proposed the CUF for the beam analyses using hierarchical displacement-based theories wherein no ad hoc assumption for transverse shear is required. Using the proposed 1D CUF, non-classical features, such as in- and out-of-plane warping of beam cross section can be adequately predicted without considering dedicated warping functions. Also, classical models, such as EBBT and TBT can be retrieved as special cases. For accurate estimation of displacement, strain and stress distribution at particular geometrical locations such as voids and corners of beams with uniform cross sections and to treat complex geometrical cross sections and loadings, Carrera *et al.* (2010) systematically implemented the FE in 1D CUF. Many works have been published to highlight the capabilities of the CUF-based 1D structural theory. Static analyses have been considered for compact and thin-walled structures in Carrera (2011a) and for bridge-like cross sections in Carrera *et al.* (2012). Free vibration analyses have been carried out on hollow cylindrical structures in Carrera *et al.* (2011b). Moreover, Carrera and Petrolo (2012b) developed a beam model with only displacement degrees of freedom (DOFs) by using Lagrange polinamials for the expansion over cross section. Mixed axiomatic/asymptotic performances have been detailed in a recent work by Carrera and Petrolo (2011). They highlighted the participation of higher-order terms of the refined beam theories for static analyses of beams with arbitrary cross sections and loadings. Free vibration studies of beams using 1D CUF have been carried out by Carrera *et al.* (2011b). A brief review of FE formulations for vibration analyses of thin/thick composite beam structures was also given. 1D beam models within the framework of CUF were capable of predicting 3D features of the vibration modes. Moreover, shell-type vibration modes for beams with annular sections were easily detected.

It is worth mentioning that the recent

literature (Turvey, 1996; Roberts and Al Ubaidi, 2001; 2002; Andrade and Camotim, 2004; Saadé *et al.*, 2004; De Lorenzis and La Tegola, 2005; Andrade *et al.*, 2007; Ascione *et al.*, 2011) consisting of the numerical, theoretical, and experimental studies pertaining to the contribution of shear deformation on buckling of thin-walled structures highlights the continuing research interests dealing with the issues of lateral as well as flexural torsional buckling of beams with arbitrary cross sections on unified basis. Ibrahim *et al.* (2012) proposed buckling analysis of composite structures by means of refined beam models. This work presents the systematic approach to the buckling analysis of beams of arbitrary cross section geometries by higher-order models using 1D formulations obtained within the framework of the CUF. Beam theories are obtained on the basis of Taylor-type and Lagrange polynomial expansions. In particular, buckling behaviour of beams with square, doubly symmetric open cross section, thin rectangular and annular cross sections are investigated and various types of bucking modes are observed. The global as well as local buckling phenomena are observed with substantial decrease in computational cost. Nonclassical features like torsional and annular modes are highlighted.

2 Advanced beam models and related finite element formulations

2.1 Framework of Carrera unified formulation

The chosen coordinate system is presented in Fig. 1. The beam boundaries over y are $0 \le y \le L$. The displacement vector is

$$\boldsymbol{u}(x,y,z) = \{u_x \quad u_y \quad u_z\}^{\mathrm{T}}, \tag{1}$$

where the superscript 'T' represents the transpose. Stress, $\boldsymbol{\sigma}$, and strain, $\boldsymbol{\epsilon}$, components can be written as

$$\begin{aligned} \boldsymbol{\sigma}_p &= \{\sigma_{zz}\ \sigma_{xx}\ \sigma_{zx}\}^{\mathrm{T}},\ \boldsymbol{\epsilon}_p = \{\epsilon_{zz}\ \epsilon_{xx}\ \epsilon_{zx}\}^{\mathrm{T}}, \\ \boldsymbol{\sigma}_n &= \{\sigma_{zy}\ \sigma_{xy}\ \sigma_{yy}\}^{\mathrm{T}},\ \boldsymbol{\epsilon}_n = \{\epsilon_{zy}\ \epsilon_{xy}\ \epsilon_{yy}\}^{\mathrm{T}}, \end{aligned} \tag{2}$$

where subscript "n" represents terms normal to the cross section, and "p" stands for terms laying on Ω. Shear strains are meant as engineering components. Linear strain-displacement relations are written as

$$\boldsymbol{\epsilon}_p = \boldsymbol{D}_p\boldsymbol{u},\ \ \boldsymbol{\epsilon}_n = \boldsymbol{D}_n\boldsymbol{u} = (\boldsymbol{D}_{n\Omega} + \boldsymbol{D}_{ny})\boldsymbol{u}, \tag{3}$$

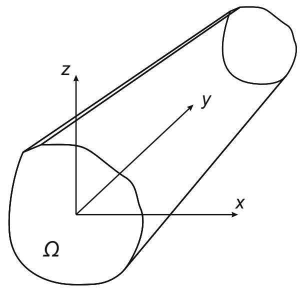

Fig. 1 Coordinate frame of the beam model

Ω: cross section domain

where

$$\begin{cases} \boldsymbol{D}_p = \begin{bmatrix} 0 & 0 & \frac{\partial}{\partial z} \\ \frac{\partial}{\partial x} & 0 & 0 \\ \frac{\partial}{\partial z} & 0 & \frac{\partial}{\partial x} \end{bmatrix}, \\ \boldsymbol{D}_{n\Omega} = \begin{bmatrix} 0 & 0 & 0 \\ 0 & \frac{\partial}{\partial x} & 0 \\ 0 & \frac{\partial}{\partial z} & 0 \end{bmatrix}, \\ \boldsymbol{D}_{ny} = \begin{bmatrix} 0 & \frac{\partial}{\partial y} & 0 \\ \frac{\partial}{\partial y} & 0 & 0 \\ 0 & 0 & \frac{\partial}{\partial y} \end{bmatrix}. \end{cases} \tag{4}$$

The Hooke law is exploited as

$$\boldsymbol{\sigma} = \widetilde{\boldsymbol{C}}\boldsymbol{\epsilon}. \tag{5}$$

According to Eq. (2), the preceding equation becomes

$$\begin{cases} \boldsymbol{\sigma}_p = \widetilde{\boldsymbol{C}}_{pp}\boldsymbol{\epsilon}_p + \widetilde{\boldsymbol{C}}_{pn}\boldsymbol{\epsilon}_n, \\ \boldsymbol{\sigma}_n = \widetilde{\boldsymbol{C}}_{np}\boldsymbol{\epsilon}_p + \widetilde{\boldsymbol{C}}_{nn}\boldsymbol{\epsilon}_n. \end{cases} \tag{6}$$

In the case of isotropic material, the matrices $\widetilde{\boldsymbol{C}}_{pp}$, $\widetilde{\boldsymbol{C}}_{nn}$, $\widetilde{\boldsymbol{C}}_{pn}$, and $\widetilde{\boldsymbol{C}}_{np}$ are

$$\begin{cases} \widetilde{\boldsymbol{C}}_{pp} = \begin{bmatrix} \widetilde{C}_{11} & \widetilde{C}_{12} & 0 \\ \widetilde{C}_{12} & \widetilde{C}_{22} & 0 \\ 0 & 0 & \widetilde{C}_{66} \end{bmatrix}, \\ \widetilde{\boldsymbol{C}}_{nn} = \begin{bmatrix} \widetilde{C}_{55} & 0 & 0 \\ 0 & \widetilde{C}_{44} & 0 \\ 0 & 0 & \widetilde{C}_{33} \end{bmatrix}, \\ \widetilde{\boldsymbol{C}}_{pn} = \widetilde{\boldsymbol{C}}_{np}^{\mathrm{T}} = \begin{bmatrix} 0 & 0 & \widetilde{C}_{13} \\ 0 & 0 & \widetilde{C}_{23} \\ 0 & 0 & 0 \end{bmatrix}. \end{cases} \tag{7}$$

For the sake of brevity, expressions relating coefficients $[\widetilde{C}]_{ij}$, Young's modulus (E), and Poisson's ratio (ν) are not reported here and can be found in existing literature (e.g., Tsai, 1988).

In the framework of the CUF, the displacement components are assumed as an expansion in terms of generic functions, F_τ:

$$\boldsymbol{u} = F_\tau \boldsymbol{u}_\tau, \qquad \tau = 1, 2, \cdots, M, \tag{8}$$

where F_τ are functions of coordinates x and z on the cross section, $\boldsymbol{u}_\tau$ is the displacement vector, and M represents the number of terms of the expansion of order N. According to the Einstein notations, the repeated subscript τ indicates summation. In the Subsections 2.2 and 2.3, advanced beam formulations using Taylor series (expansion for cross sectional displacement coupled with FEs representing the translational displacement field) and Lagrange polynomials are discussed.

2.2 Taylor 1D CUF

Using the Maclaurin expansion that uses as base the 2D polynomials $x^i z^j$, where i and j are positive integers and considering the expansion up to the quadratic terms, Eq. (8) can be written as

$$\begin{cases} u_x = u_{x_1} + x u_{x_2} + z u_{x_3} + x^2 u_{x_4} + xz u_{x_5} + z^2 u_{x_6}, \\ u_y = u_{y_1} + x u_{y_2} + z u_{y_3} + x^2 u_{y_4} + xz u_{y_5} + z^2 u_{y_6}, \\ u_z = u_{z_1} + x u_{z_2} + z u_{z_3} + x^2 u_{z_4} + xz u_{z_5} + z^2 u_{z_6}. \end{cases} \tag{9}$$

Note that the quadratic model is reported as an example and that any order models can be obtained. The Timoshenko beam model can be obtained by acting on the F_τ expansion. Two conditions have to be imposed.

(1) A first-order approximation kinematic field:

$$\begin{cases} u_x = u_{x_1} + x u_{x_2} + z u_{x_3}, \\ u_y = u_{y_1} + x u_{y_2} + z u_{y_3}, \\ u_z = u_{z_1} + x u_{z_2} + z u_{z_3}. \end{cases} \tag{10}$$

(2) The displacement components u_x and u_z have to be constant above the cross section:

$$u_{x_2} = u_{z_2} = u_{x_3} = u_{z_3} = 0. \tag{11}$$

The Euler-Bernoulli beam model can be obtained through the penalization of ϵ_{xy} and ϵ_{zy}. This condition can be imposed using a penalty value χ in the following constitutive relation:

$$\begin{cases} \sigma_{xy} = \chi \widetilde{C}_{55} \epsilon_{xy} + \chi \widetilde{C}_{45} \epsilon_{zy}, \\ \sigma_{zy} = \chi \widetilde{C}_{45} \epsilon_{xy} + \chi \widetilde{C}_{44} \epsilon_{zy}. \end{cases} \tag{12}$$

Unless specified otherwise, for classical (EBBT and TBT) and first-order models, Poisson's locking is corrected according to Carrera and Giunta (2010).

2.3 Lagrange 1D CUF

In this section Lagrange polynomials are used to describe the cross section displacement field. Nine-point, L9, polynomials are adopted in this study whose explicit expressions can be written as

$$F_\tau = \begin{cases} \frac{1}{4}(r^2 + r\, r_\tau)(s^2 + s\, s_\tau), & \tau = 1, 3, 5, 7, \\ \frac{1}{2} s_\tau^2 (s^2 - s\, s_\tau)(1 - r^2) \\ \quad + \frac{1}{2} r_\tau^2 (r^2 - r\, r_\tau)(1 - s^2), & \tau = 2, 4, 6, 8, \\ (1 - r^2)(1 - s^2), & \tau = 9, \end{cases} \tag{13}$$

where r and s are from -1 to 1. Fig. 2 and Table 1 show the point locations and natural coordinates, respectively.

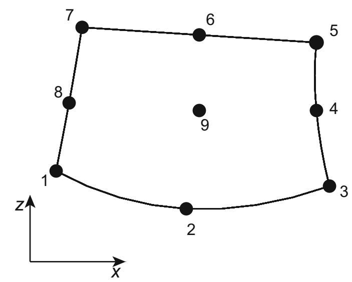

Fig. 2 A nine-point L9 cross section element

Table 1 Nine-point L9 cross section element point natural coordinates

Point	r_τ	s_τ	Point	r_τ	s_τ
1	−1	−1	6	0	1
2	0	−1	7	−1	1
3	1	−1	8	−1	0
4	1	0	9	0	0
5	1	1			

The displacement field given by an L9 element is

$$\begin{cases} u_x = F_1 u_{x_1} + F_2 u_{x_2} + F_3 u_{x_3} + F_4 u_{x_4} + \cdots + F_9 u_{x_9}, \\ u_y = F_1 u_{y_1} + F_2 u_{y_2} + F_3 u_{y_3} + F_4 u_{y_4} + \cdots + F_9 u_{y_9}, \\ u_z = F_1 u_{z_1} + F_2 u_{z_2} + F_3 u_{z_3} + F_4 u_{z_4} + \cdots + F_9 u_{z_9}, \end{cases} \tag{14}$$

where $u_{x_1}, u_{x_2}, \cdots, u_{z_9}$ are the displacement variables of the problem and they represent the translational displacement components of each of the nine points of the L9 element. The cross section can be discretized by means of several L-elements. Fig. 3 shows the assembly of two L9 that share a common edge with three points. A more detailed description of the CUF Lagrange 1D formulation can be found in Carrera and Petrolo (2012a; 2012b).

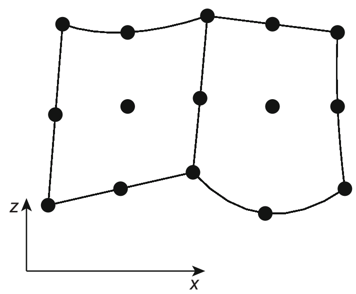

Fig. 3 Two assembled nine-point L9 elements

2.4 Finite element implementation and stiffness matrix

Introducing the shape functions, N_i, and the nodal displacement vector, $\boldsymbol{q}_{\tau i}$:

$$\boldsymbol{q}_{\tau i}=\left\{q_{u_{x_{\tau i}}} \ \ q_{u_{y_{\tau i}}} \ \ q_{u_{z_{\tau i}}}\right\}^{\mathrm{T}}, \tag{15}$$

the displacement vector becomes

$$\boldsymbol{u}_{\tau}=N_i F_{\tau} \boldsymbol{q}_{\tau i}, \tag{16}$$

where shape functions N_i are standard shape functions taken from Bathe (1996). Elements with 3 and 4 nodes (B3 and B4), that is, quadratic and cubic approximations along the y axis are adopted, respectively. It is to be noted that the order of the beam model and the approximation along the longitudinal axis are completely independent to each other. An N-order beam model is therefore a theory that exploits an N-order polynomial to describe the kinematics of the cross section.

The stiffness matrix of the elements and the external loadings, are obtained via the principle of virtual displacement (PVD):

$$\delta L_{\mathrm{int}}=\int_V\left(\delta \boldsymbol{\epsilon}_p^{\mathrm{T}} \boldsymbol{\sigma}_p+\delta \boldsymbol{\epsilon}_n^{\mathrm{T}} \boldsymbol{\sigma}_n\right) \mathrm{d} V=\delta L_{\mathrm{ext}}, \tag{17}$$

where L_{int}, L_{ext}, and δ represent the internal work, work of the external loadings, and the virtual variation, respectively. Using Eqs. (3), (6), and (16), the virtual variation of the internal work is rewritten in a compact format as

$$\delta L_{\mathrm{int}}=\delta \boldsymbol{q}_{\tau i}^{\mathrm{T}} \boldsymbol{K}^{i j \tau s} \boldsymbol{q}_{s j}, \tag{18}$$

where $\boldsymbol{K}^{ij\tau s}$ stands for the stiffness matrix in the form of the fundamental nucleus. The first component of the fundamental nucleus can be written as

$$\begin{aligned} K_{xx}^{ij\tau s}= & \widetilde{C}_{22} \int_{\Omega} F_{\tau,_x} F_{s,_x} \mathrm{d} \Omega \int_l N_i N_j \mathrm{d} y \\ & +\widetilde{C}_{66} \int_{\Omega} F_{\tau,_z} F_{s,_z} \mathrm{d} \Omega \int_l N_i N_j \mathrm{d} y \\ & +\widetilde{C}_{44} \int_{\Omega} F_{\tau} F_s \mathrm{d} \Omega \int_l N_{i,_y} N_{j,_y} \mathrm{d} y . \end{aligned} \tag{19}$$

The detailed expansion of fundamental nucleus can be seen in Carrera and Giunta (2010). Using 1D CUF, it is possible to obtain hierarchical higher-order beam models without changing the expression of the nucleus components. The shear locking is corrected through the selective integration technique (Bathe, 1996). In Carrera *et al.* (2011a), more details on the beam model considered in this work can be found.

3 Governing equations for linearized stability analysis

The buckling equations are obtained according to Euler's method of adjacent equilibrium states. It consists of a linearized stability analysis with the following assumptions:

1. The prebuckling deformation is neglected.
2. The initial stress $\boldsymbol{\sigma}^0$ remains constant during buckling (i.e., it neither varies in magnitude nor in direction).
3. At bifurcation, the equilibrium states are infinitesimally adjacent so that a linearization is possible.

The buckling load can then be defined via a scalar load factor λ as the load $\boldsymbol{\sigma}=\lambda \boldsymbol{\sigma}^0$ for which an equilibrium configuration $\boldsymbol{u} \neq \mathbf{0}$ exists such that

$$\delta \boldsymbol{u}^{\mathrm{T}}\left[\boldsymbol{K}+\lambda \boldsymbol{K}_{\sigma}\left(\boldsymbol{\sigma}^0\right)\right] \boldsymbol{u}=\mathbf{0}, \tag{20}$$

where $\boldsymbol{K}$ is the linear stiffness matrix and $\boldsymbol{K}_\sigma$ is the geometric stiffness matrix which is obtained using the following expression:

$$\delta L_{nl}=\int_{\Omega} \int_l \delta \epsilon_{yy}^{nl} \sigma_{yy}^0 \mathrm{d} y \mathrm{d} \Omega, \tag{21}$$

where σ_{yy}^0 is the actual initial stress, and $\delta\epsilon_{yy}^{nl}$ are virtual nonlinear direct in-plane strains that can be expressed as

$$\epsilon_{yy}^{nl} = \frac{1}{2}\left(u_{y,y}^2 + u_{y,y}^2 + u_{y,y}^2\right), \tag{22}$$

and the non-zero terms of the geometric stiffness matrix $\boldsymbol{K}_\sigma$ can be written as

$$\begin{aligned} K_{\sigma_{xx}}^{ij\tau s} =& K_{\sigma_{yy}}^{ij\tau s} = K_{\sigma_{zz}}^{ij\tau s} = \\ =& \int_\Omega F_\tau F_s \mathrm{d}\Omega \int_l N_{i,y} N_{j,y} \mathrm{d}y. \end{aligned} \tag{23}$$

4 Numerical analysis and discussion

4.1 Square compact section beam

Validation of the present approach is carried out considering simply supported beam with a square cross section. Geometrical and material properties are: length to thickness ratio $L/a = 20$, where L is the length of the beam and a is the side of the square section and is considered equal to 1 m; Young's modulus $E = 71.7$ GPa; Poisson's ratio $\nu = 0.3$. The results are compared with that of Matsunaga (1996) and FEM results generated by ANSYS. Based on the convergence study, the beam is modeled in ANSYS using B3 elements with 20 divisions along length. Note that the torsional buckling loads are not obtained in ANSYS using B3 elements. Table 3 presents the first three buckling loadings for bending, torsion and axial modes using the third order models with 20 B3 elements in longitudinal directions. It can be noted that $N = 2$ model gives a higher bending buckling load than $N = 1$. It is important to underline that this is due to the Poisson locking correction that artificially improve the linear solution (Carrera and Giunta, 2010). The present results are in good agreement with those obtained using ANSYS for the first three critical loads in bending as well with those given in Matsunaga (1996).

A comparative study on the effects of boundary conditions and the aspect ratios of beams with square cross section is carried out (Table 3). In general, the first 20 modes of the different beams considered are dominated by the bending buckling modes. For the case of clamped-free ($L/a = 10$) and clamped-clamped ($L/a = 10$) beams, least numbers (one and two, respectively) of modes with localized axial buckling effects are depicted. For the case of clamped-clamped ($L/a = 5$) and hinged-hinged ($L/a = 10$), pairs of modes (Modes 5 and 6; Modes 11 and 12, respectively) depicting a twisting type buckling behavior are also observed. Moreover, the effect of change in aspect ratio on higher bending type modes is more pronounced than that on lower bending modes.

To highlight the capabilities of the present refined beam models, the first three pure torsional modes for clamped-clamped and hinged-hinged beams with $L/a = 5$ and 10 are plotted in Figs. 4 and 5, respectively. It can be seen that the present model is effective in predicting the 3D features like the torsional buckling, as it is pretty clear that modes having cross sections distorted can also be captured easily. It is interesting to observe that the effect of boundary constraints is more pronounced for the beams with slender cross sections ($L/a = 10$).

4.2 I-section beam

In this section, doubly symmetric beam with an open cross section (I-section beam) is considered

Table 2 Bending, torsion, and axial dimensionless buckling loads ($P = P_o(12/\pi^2)(L/a)^2/E$, where P_o is the actual buckling load) for an isotropic beam with a length to thickness ratio of 20

Model	Dimensionless buckling load								
	Bending			Torsion			Axial		
	$m=1$	$m=2$	$m=3$	$m=1$	$m=2$	$m=3$	$m=1$	$m=2$	$m=3$
FEM (ANSYS)	1.0000	4.000	9.000	–	–	–	–	–	–
Matsunaga (1996)	0.9919	3.873	8.387	–	–	–	486.25	485.98	485.51
EBBT	0.9950	3.956	8.813	–	–	–	483.98	484.98	484.98
TBT	0.9900	3.875	8.422	–	–	–	481.18	481.18	481.19
N=1	0.9925	3.884	8.437	182.84	182.84	182.84	486.34	486.94	488.74
N=2	0.9927	3.885	8.444	182.84	182.84	182.84	484.70	485.52	489.68
N=3	0.9918	3.873	8.387	182.84	182.84	182.84	483.21	484.76	485.56

FEM: finite element method; EBBT: Euler-Bernoulli beam theory; TBT: Timoshenko beam theory; m: mode number

Table 3 Comparison of first ten pairs of non-dimensional buckling loads using ten B4 elements ($P = P_o(12/\pi^2)(L/a)^2/E$, where P_o is the actual buckling load) for beams with different boundary conditions and aspect ratios

P	Non-dimensional buckling load							
	Clamped-clamped		Clamped-hinged		Clamped-free		Hinged-hinged	
	$L/a=5$	$L/a=10$	$L/a=5$	$L/a=10$	$L/a=5$	$L/a=10$	$L/a=5$	$L/a=10$
P_1	0.466[a]	4.789	0.467[a]	2.319	0.273	0.318	0.888	0.968
P_2	0.467[a]	4.789	1.712	2.319	0.273	0.318	0.888	0.968
P_3	2.961	8.098	1.712	5.741	0.467[a]	2.517	2.667	3.529
P_4	2.961	8.098	3.106[a]	5.741	1.887	2.517	2.667	3.529
P_5	2.984[t]	12.429	3.323	7.541	1.887	5.921	3.334	6.748
P_6	3.219[t]	12.429	3.323	7.541	2.984[a]	5.921	3.334	6.748
P_7	3.833	15.589	3.538	8.507[a]	3.659	9.704	3.343	7.514[a]
P_8	3.833	15.589	3.538	9.699	3.659	9.704	3.343	7.622[a]
P_9	4.467	16.487[a]	3.639[a]	9.699	4.453	13.388	3.639[a]	7.851[a]
P_{10}	4.467	16.589[a]	4.444	13.372	4.453	13.388	3.639[a]	7.939[a]
P_{11}	4.891	19.029	4.444	13.372	5.270	16.487[a]	4.461	8.389[t]
P_{12}	4.891	19.029	5.308	16.529[a]	5.270	16.748	4.461	8.625[t]
P_{13}	6.014	21.481	5.308	16.737	6.089[a]	16.748	5.779	10.890
P_{14}	6.014	21.481	5.921[a]	16.737	6.276	19.712	5.779	10.890
P_{15}	6.707	24.049	6.342	19.726	6.276	19.712	5.921[a]	14.429
P_{16}	6.707	24.049	6.342	19.726	6.937	22.285	5.921[a]	14.429
P_{17}	7.542	25.869	6.380[a]	22.292	6.937	22.285	6.380[a]	17.657
P_{18}	7.542	25.869	7.164	22.292	7.203[a]	24.501	6.380[a]	17.657
P_{19}	7.914	27.782	7.164	23.392[a]	7.211[a]	24.501	6.765	20.499
P_{20}	7.914	27.782	7.750	24.537	7.270[a]	26.406	6.765	20.499

[a] Axial mode; [t] Torsional mode

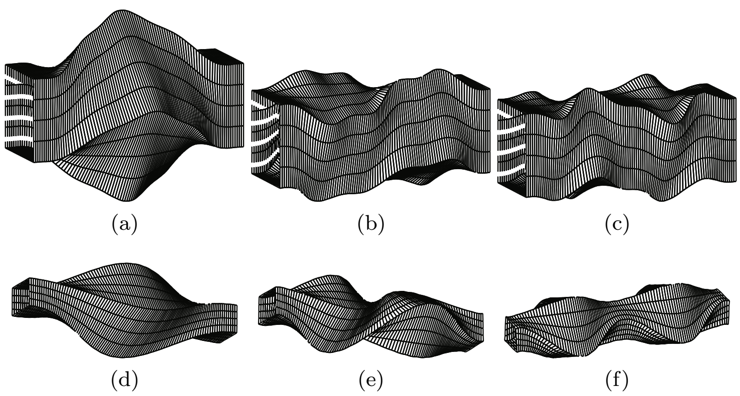

Fig. 4 First three torsional modes for clamped-clamped boundary conditions for different aspect ratios

(a) $L/a=5$, $P_{44}=9.867$; (b) $L/a=5$, $P_{45}=9.870$; (c) $L/a=5$, $P_{46}=9.870$; (d) $L/a=10$, $P_{67}=39.440$; (e) $L/a=10$, $P_{68}=39.463$; (f) $L/a=10$, $P_{69}=39.475$

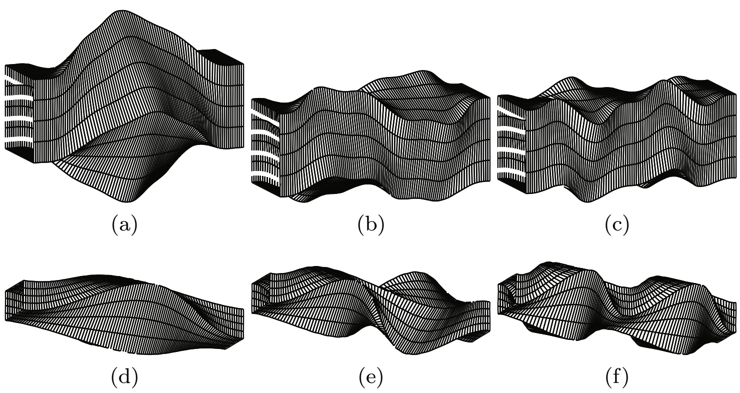

Fig. 5 First three torsional modes for simply supported boundary conditions for different aspect ratios

(a) $L/a=5$, $P_{47}=9.867$; (b) $L/a=5$, $P_{48}=9.870$; (c) $L/a=5$, $P_{49}=9.870$; (d) $L/a=10$, $P_{76}=39.442$; (e) $L/a=10$, $P_{77}=39.465$; (f) $L/a=10$, $P_{78}=39.476$

to observe the local and global buckling phenomena associated with torsional buckling. A beam can buckle out of plane if it does not have sufficient lateral stiffness and is termed as lateral buckling. This phenomenon is generally accompanied with lateral deflection and a small twist without the change in the cross sectional shape. Local buckling phenomenon can also be observed if a beam buckles locally over a short length of the member with only minor changes in cross sectional shapes (Samanta and Kumar, 2006). Note that the warping, out- and in-plane deformations, torsion-bending coupling as well as distortional buckling modes are not generally observed in analyses based on classical theories. A simply supported I-beam is considered with the following geometrical properties: width of top/bottom flange = 0.21 m; thickness of top/bottom flange = 0.02 m; thickness of web = 0.012 m; overall height of the beam section = 0.6 m; length of beam = 5 m. First ten modes for the I-beam are given in Table 4 for different theories and expansion orders using ten B4 elements. For the case of classical beam theories (EBBT and TBBT) and for $N=1$, only the bending buckling modes are observed. However, for the case of $N=2$, torsional mode also appeared (Mode 10). Further refined theory (i.e., $N=3$) enables us to obtain the torsional as well as distortional modes (Fig. 6). It is clear from Fig. 6a that this mode depicts the initiation of the torsional buckling. The web remains straight but twisted almost through out its length. It is observed from Fig. 6b that the distortions in the next higher mode (Mode 11) is observed both in the longitudinal and transverse axes of the beam, and the displacement variations are observed both in the flanges and the web. Next higher modes plotted in Figs. 6c–6f depict the higher torsional buckling modes wherein prominent wave-like features exist both in the flanges as well as in the web. A comparisons with a 2D model performed with Nastran has been provided. By considering a refined 2D model with 25 000 DOFs, the results show that the first critical load is 58.84 N/m^2; and the second is 205.83 N/m^2, compared with the results from a third order model (Table 4), it is possible to see that the difference between the two solutions is 3.4% for the first critical load and 9.2% for the second. While the first load is well predicted by the third order model, for the higher critical loads a more refined model should be used.

Table 4 First ten buckling loads for different refined beam theories using ten B4 elements for simply supported I-section beam

Model	Critical load ($\times 10^6$ N/m^2)									
	P_1	P_2	P_3	P_4	P_5	P_6	P_7	P_8	P_9	P_{10}
EBBT	57.89	231.06	518.22	918.07	1430.19	1614.52	2055.97	2799.01	3663.73	4641.99
TBT	57.77	229.11	508.36	886.91	1354.27	1527.10	1899.25	2510.99	3179.79	3896.91
$N=1$	57.77	229.11	508.36	886.91	1354.27	1527.10	1899.25	2510.99	3179.79	3896.91
$N=2$	57.93	231.36	517.98	911.70	1402.54	1527.26	1978.06	2625.36	3331.39	3943.11
$N=3$	57.88	230.57	514.23	900.49	1376.46	1455.98	1926.36	2533.69	3183.12	3367.46
$N=4$	56.83	224.66	495.68	813.98	857.98	1010.90	1297.04	1328.62	1457.72	1753.00

EBBT: Euler-Bernoulli beam theory; TBT: Timoshenko beam theory

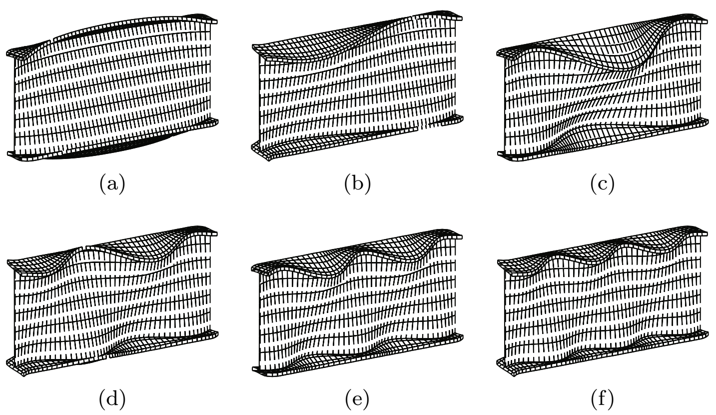

Fig. 6 Torsional and distortional buckling of simply supported I-beam
(a) P_{10}=3367.46 MPa; (b) P_{11}=3606.44 MPa; (c) P_{13}=4054.13 MPa; (d) P_{15}=4472.06 MPa; (e) P_{17}=5017.50 MPa; (f) P_{19}=5621.91 MPa

4.3 Thin rectangular section beam (plate)

Buckling of beams with very thin rectangular cross section is studied in this section. Two different models have been used for such analysis. The first is based on Taylor expansion (TE), and the second is based on the Lagrange function(LE).

A simply supported beam with a thin rectangular cross section has been investigated using the TE approach. The dimensions are: width, $a = 2.0$ m; length, $L = 2.0$ m; thikness, $h = 0.01$ m. First six buckling modes are presented in Table 5 for different theories using ten B4 elements. It can be observed that the first six bending buckling modes obtained using the refined theory with expansion order higher than $N = 2$ match very well with that of NASTRAN. Modes 1, 3, and 5 are bending modes. Modes 2, 4, and 6 are torsional modes. For each model, the DOFs involved in the solution are reported. The results show that the higher-order beam model provide results comparable with those by commercial code in significantly reducing the DOFs.

The shell capabilities of the present 1D LE are investigated here through the analysis of a simply supported thin plate. The length of the plate is 0.1 m, the width is 0.025 m, and the thickness is 0.001 m. An isotropic material is adopted having $E = 71.7$ GPa and $\nu = 0.3$. Results are compared with those from a shell model in NASTRAN and from 1D CUF model closed-form Navier-type solutions. These results are taken from Carrera *et al.* (2011a). 1D Lagrange CUF models are adopted with two cross section meshes: 1 L9 and 3 L9. The latter has the L9 elements spread along the width direction. A ten element B4 mesh is used along the longitudinal direction.

Table 6 presents the bending and torsional buckling loads of the present plate. The second column shows the number of DOFs of each FEM model. Third and seventh order Taylor models are considered for the closed-form solution. Fig. 7 presents the fourth torsional buckling mode, whereas Fig. 8 shows a shell-like mode affected by severe cross section distortions.

4.4 Annular circular section beam

In this section, buckling analysis of beam with annular cross section is presented. A beam with clamped boundary conditions (all DOFs clamped at near end and all clamped but $u_y \neq 0$ at far end) is considered with the following section dimensions: outer radius of the section =1.0 m; inner radius =

Table 5 First six buckling loads for different refined beam theories using ten B4 elements for simply supported thin rectangular section beam

Model	DOFs	Critical load ($\times10^6$ N/m^2)					
		P_1	P_2	P_3	P_4	P_5	P_6
EBBT	279	1.47	5.90	13.27	23.58	36.84	53.07
TBT	279	1.47	5.89	13.26	23.56	36.80	52.97
$N = 1$	279	1.47	5.90	13.26	23.56	36.80	52.97
$N = 2$	558	1.62	4.74	6.48	10.69	14.57	20.59
$N = 3$	930	1.55	4.42	6.38	9.38	14.47	17.40
$N = 4$	1395	1.55	4.43	6.37	9.44	14.45	17.41
2D Nastran	8200	1.56	4.28	6.43	9.22	14.06	17.54
3D Nastran	25 010	1.56	4.29	6.45	9.25	14.68	17.65

EBBT: Euler-Bernoulli beam theory; TBT: Timoshenko beam theory; DOFs: degrees of freedom

Table 6 First four bending and torsional buckling loadings for the thin plate

Model		DOFs	Buckling load (MPa)							
			Bending				Torsion			
			1	2	3	4	1	2	3	4
Shell		51000	5.932	24.03	54.76	98.25	181.61	198.78	229.16	272.31
1D CUF FEM	1 L9	1893	5.934	24.08	54.98	98.85	182.31	201.45	233.25	277.66
	3 L9	837	5.934	24.06	54.85	98.47	181.41	200.46	232.12	276.28
1D CUF ANLT	$N = 3$	–	5.934	24.08	54.98	98.85	181.18	201.09	232.74	277.00
	$N = 7$	–	5.932	24.03	54.71	98.08	180.38	198.88	229.68	272.72

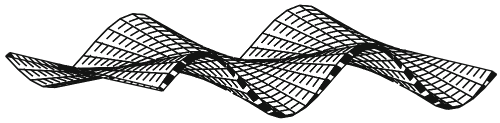

Fig. 7 Fourth torsional buckling mode

$P = 276.28$ MPa, 3 L9 model

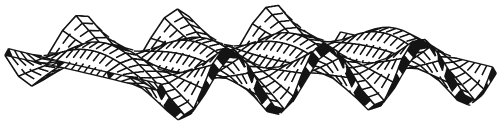

Fig. 8 Shell-like bucking mode

$P = 1410.5$ MPa, 3 L9 model

0.99 m; length = 10 m. Comparison of shell modes obtained using NASTRAN and the present theory is carried out and it can be observed from Table 7 and Fig. 9 that the second and sixth modes obtained using the present theory with expansion order $N = 7$ match very well with that of obtained through NASTRAN shell, both in mode shape as well as in magnitude. Also it is clear from Table 7 that the circumferential modes are obtained with a significantly lower computational cost as the DOFs of refined theory with $N = 7$ are more than three times less than that of NASTRAN shell. First twelve buckling modes obtained using different theories and expansion orders are given in Table 8. Using the EBBT and TBT, and the refined theory with lower order of expansion (up to $N = 2$), only the bending buckling modes are depicted. With an increase in the expansion ($N = 3$), crude circumferential modes with overestimated values of buckling loads start to appear. The positions of the first twelve critical buckling loads are plotted for different beam models in Fig. 10. It is interesting to note that the circumferential modes appear even before the bending modes for expansion orders greater than three. Also for $N = 4$, circumferential modes with two lobes are observed and with a further increase of expansion order, circumferential modes with more than two lobes are obtained. Accurately estimated critical loads for buckling modes with higher than two lobes are easily depicted with $N = 7$. Modes with three (Mode 9) and four lobes (Mode 13) are plotted in Fig. 11 and the deformed three and four lobed cross sections at mid length of the shell can be observed.

Table 7 Comparison between NASTRAN shell and present beam elements solution for the first and third buckling modes (clamped annular cross section beam, $L/d = 10$)

RBT	DOFs	Critical load ($\times 10^8$ N/m^2)	
		First buckling mode	Third buckling mode
NS	10 380	6.25	8.51
Present beam	3348	6.23	8.29

RBT: refined beam theory; DOFs: degrees of freedom; NS: NASTRAN shell

5 Conclusions

Analysis of beams has been carried out using the refined beam theories by successfully employing the 1D CUF, which permits us to deal with any-order of beam theories without need of ad hoc implementations. Advanced theories are obtained based on Taylor series and Lagrange polynomials. The element stiffness is obtained in a compact form which is independent of the theory approximation order assumed

Table 8 First ten buckling loads for different refined beam theories using ten B4 elements for annular circular section beam

Model	DOFs	Critical load ($\times 10^9$ N/m^2)											
		P_1	P_2	P_3	P_4	P_5	P_6	P_7	P_8	P_9	P_{10}	P_{11}	P_{12}
EBBT	279	1.732^b	1.733^b	4.888^b	4.889^b	9.121^b	9.134^b	13.994^b	14.045^b	19.115^b	19.251^b	24.183^b	24.469^b
TBT	279	1.648^b	1.700^b	4.224^b	4.335^b	7.073^b	7.223^b	9.784^b	9.950^b	12.189^b	12.356^b	14.259^b	14.418^b
$N = 1$	279	1.700^b	1.700^b	4.334^b	4.335^b	7.222^b	7.223^b	9.949^b	9.950^b	12.356^b	12.356^b	14.418^b	14.420^b
$N = 2$	558	1.759^b	1.760^b	4.431^b	4.432^b	7.338^b	7.339^b	10.072^b	10.073^b	12.484^b	12.487^b	14.548^b	14.553^b
$N = 3$	930	1.620^b	1.620^b	3.690^b	3.750^b	4.324^c	4.340^c	4.651^c	4.673^c	5.069^b	5.366^b	5.600^b	5.600^b
$N = 4$	1395	0.925^c	0.926^c	1.134^c	1.145^c	1.161^c	1.407^c	1.491^c	1.527^c	1.664^c	1.666^b	1.666^b	1.811^c
$N = 5$	1953	0.722^c	0.727^c	0.975^c	0.986^c	0.990^c	1.132^c	1.203^c	1.204^c	1.248^c	1.250^c	1.250^c	1.255^c
$N = 6$	2604	0.695^c	0.698^c	0.715^c	0.734^c	0.839^c	0.872^c	0.874^c	0.961^c	0.964^c	0.970^c	0.993^c	0.993^c
$N = 7$	3348	0.616^c	0.623^c	0.640^c	0.640^c	0.823^c	0.829^c	0.831^c	0.833^c	0.923^c	0.959^c	0.962^c	0.986^c

^{b} Bending mode; ^{c} Circumferential mode; EBBT: Euler-Bernoulli beam theory; TBT: Timoshenko beam theory; DOFs: degrees of freedom

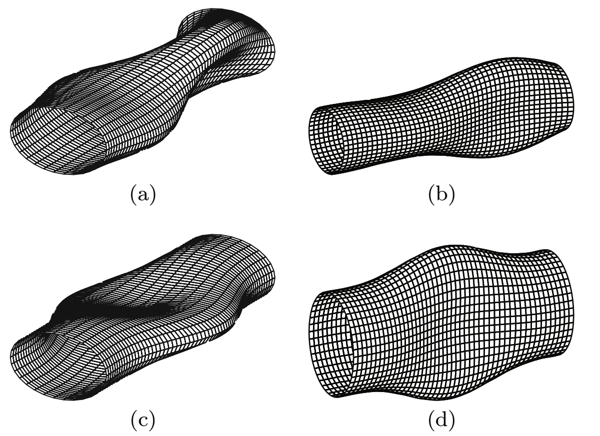

Fig. 9 Comparison of the modes obtained using present beam theory ($N=7$) and NASTRAN

(a) NASTRAN shell, $P = 6.25\times10^8$ N/m^2; (b) $N=7$, $P_2 = 6.23\times10^8$ N/m^2; (c) NASTRAN shell, $P=8.51\times10^8$ N/m^2; (d) $N=7$, $P_6 = 8.29\times10^8$ N/m^2

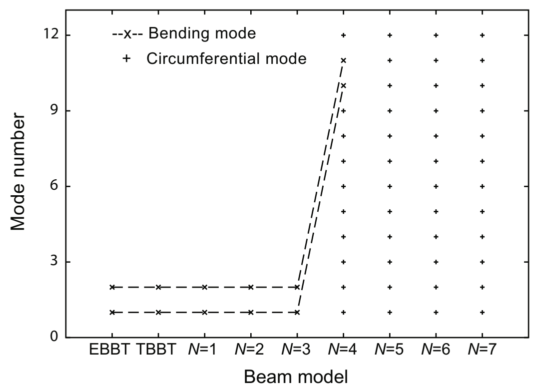

Fig. 10 Bucking modes versus beam models for annular cross section beam

as a free parameter. Evaluation of the present formulation has been carried out for the buckling analyses of beams with different cross sections. Beams with square cross section, I-sections, very thin rectangular cross sections (plate) as well as annular cross section beams (shell) with different boundary conditions have been studied. Buckling loads corresponding to the bending, axial, torsional, and distortional modes have been obtained. The present analysis carried out using the 1D theories matches very well with that of commercially available FE softwares using shell elements. The following conclusions can be drawn from the present study:

1. The present formulation gives us flexibility to deal with beam having arbitrary cross sections.

2. The torsional, distortional modes, as well as global and local buckling features are easily depicted.

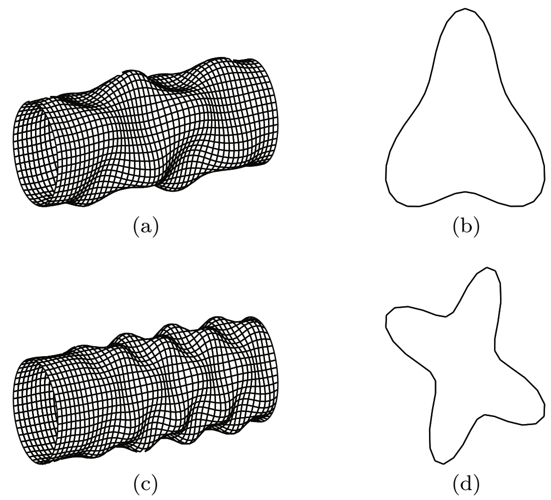

Fig. 11 Three and four lobed modes and the corresponding cross sections at midlength of annular cross section beams

(a) Three lobed mode, $P_9 = 9.226\times10^8$ N/m^2; (b) Deformed cross section of (a) at midlength; (c) Four lobed mode, $P_{13} = 9.933\times10^8$ N/m^2; (d) Deformed cross section of (c) at midlength

3. 3D features like modes wherein components of out of plane deformations are substantial can be easily obtained.

4. For the case of thin rectangular beam sections, accurate estimation of the buckling loads, as well as the corresponding mode shapes can be observed by using theory order as low as $N=2$.

5. Localized buckling effects, which can not be obtained using the classical theories like EBBT and TBT are easily obtained.

6. A general good match is found between the 1D model and the shell one for the analysed cases of plates and circumferentially complete shells.

7. The 1D Lagrange model results provide accuracies lying in between those from a third and seventh order Taylor model for the case of plate structures.

8. The present formulation is able to detect shell-like modes with a substantial decrease in computational cost. Shell-like features like circumferential modes are exactly matched with that of commercially available finite element software using only ten B4 elements and considering $N=7$.

Future investigations involving the refined beam theories based on CUF could be directed towards considering the nonlinear analysis of structures.

References

Andrade, A., Camotim, D., 2004. Lateral-torsional buckling of prismatic and tapered thin-walled open beams:

assessing the influence of pre-buckling deflections. *Steel and Composite Structures*, **4**(4):281-300.

Andrade, A., Camotim, D., Dinis, P.B., 2007. Lateral-torsional buckling of singly symmetric web-tapered thin-walled I-beams: 1D model vs. shell FEA. *Computers & Structures*, **85**(17-18):1343-1359. [doi:10.1016/j.compstruc.2006.08.079]

Ascione, L., Giordano, A., Spadea, S., 2011. Lateral buckling of pultruded FRP beams. *Composites Part B Engineering*, **42**(4):819-824. [doi:10.1016/j.compositesb.2011.01.015]

Bathe, K.J., 1996. Finite Element Procedures. Prentice Hall, Englewood Cliffs, NJ.

Bebiano, R., Silvestre, N., Camotim, D., 2008. Local and global vibration of thin-walled members subjected to compression and non-uniform bending. *Journal of Sound and Vibration*, **315**(3):509-535. [doi:10.1016/j.jsv.2008.02.036]

Berdichevsky, V., Armanios, E., Badir, A., 1992. Theory of anisotropic thin-walled closed-cross-section beams. *Composites Engineering*, **2**(5-7):411-432. [doi:10.1016/0961-9526(92)90035-5]

Carrera, E., 1995. A class of two dimensional theories for multilayered plates analysis. *Atti Accademia delle Scienze di Torino, Memorie Scienze Fisiche*, **19-20**:49-87.

Carrera, E., 2000. Single- vs. multilayer plate modellings on the basis of Reissner's mixed theorem. *AIAA Journal*, **38**(2):342-352. [doi:10.2514/2.962]

Carrera, E., 2003. Theories and finite elements for multilayered plates and shells: a unified compact formulation with numerical assessment and benchmarking. *Archives of Computational Methods in Engineering*, **10**(3):215-296. [doi:10.1007/BF02736224]

Carrera, E., Demasi, L., 2002. Classical and advanced multilayered plate elements based upon PVD and RMVT: Part 1—Derivation of finite element matrices. *International Journal for Numerical Methods in Engineering*, **55**(2):191-231. [doi:10.1002/nme.492]

Carrera, E., Giunta, G., 2009. Hierarchical evaluation of failure parameters in composite plates. *AIAA Journal*, **47**(3):692-702. [doi:10.2514/1.38585]

Carrera, E., Giunta, G., 2010. Refined beam theories based on a unified formulation. *International Journal of Applied Mechanics*, **2**(1):117-143. [doi:10.1142/S1758825110000500]

Carrera, E., Petrolo, M., 2011. On the effectiveness of higher-order terms in refined beam theories. *Journal of Applied Mechanics*, **78**(2):021013. [doi:10.1115/1.4002207]

Carrera, E., Petrolo, M., 2012a. An advanced one-dimensional formulation for laminated structure analysis. *AIAA Journal*, **50**(1):176-189. [doi:10.2514/1.J051219]

Carrera, E., Petrolo, M., 2012b. Refined beam elements with only displacement variables and plate/shell capabilities. *Meccanica*, **47**(3):537-556. [doi:10.1007/s11012-011-9466-5]

Carrera, E., Giunta, G., Nali, P., Petrolo, M, 2010. Refined beam elements with arbitrary cross-section geometries. *Computers & Structures*, **88**(5-6):283-293. [doi:10.1016/j.compstruc.2009.11.002]

Carrera, E., Giunta, G., Petrolo, M., 2011a. Beam Structures: Classical and Advanced Theories, 1st Ed. Wiley, West Sussex, UK. [doi:10.1002/9781119978565]

Carrera, E., Petrolo, M., Nali, P., 2011b. Unified formulation applied to free vibrations finite element analysis of beams with arbitrary section. *Shock and Vibration*, **18**(3):485-502. [doi:10.3233/SAV-2010-0528]

Carrera, E., Petrolo, M., Zappino, E., 2012. Performance of CUF approach to analyze the structural behavior of slender bodies. *Journal of Structural Engineering*, **138**(2):285-298. [doi:10.1061/(ASCE)ST.1943-541X.0000402]

Cowper, G.R., 1966. The shear coefficient in Timoshenko's beam theory. *Journal of Applied Mechanics*, **33**(2):335-340. [doi:10.1115/1.3625046]

De Lorenzis, L., La Tegola, A., 2005. Effect of the actual distribution of applied stresses on global buckling of isotropic and transversely isotropic thin-walled members: theoretical analysis. *Composite Structures*, **68**(3):339-348. [doi:10.1016/j.compstruct.2004.03.027]

Demasi, L., 2009. ∞^6 mixed plate theories based on the generalized unified formulation. Part I: governing equations. *Composite Structures*, **87**(1):1-11. [doi:10.1016/j.compstruct.2008.07.013]

Dong, S.B., Kosmatka, J.B., Lin, H.C., 2001. On Saint-Venant's problem for an inhomogeneous, anisotropic cylinder—Part I: methodology for Saint-Venant solutions. *Journal of Applied Mechanics*, **68**(3):376-381. [doi:10.1115/1.1363598]

Dong, S.B., Alpdongan, C., Taciroglu, E., 2010. Much ado about shear correction factors in Timoshenko beam theory. *International Journal of Solids and Structures*, **47**(13):1651-1665. [doi:10.1016/j.ijsolstr.2010.02.018]

D'Ottavio, M., Carrera, E., 2010. Variable-kinematics approach for linearized buckling analysis of laminated plates and shells. *AIAA Journal*, **48**(9):1987-1996. [doi:10.2514/1.J050203]

El Fatmi, R., 2002. On the structural behavior and the Saint Venant solution in the exact beam theory. Application to laminated composite beams. *Computers & Structures*, **80**(16-17):1441-1456. [doi:10.1016/S0045-7949(02)00090-1]

El Fatmi, R., 2007a. Non-uniform warping including the effects of torsion and shear forces. Part I: a general beam theory. *International Journal of Solids and Structures*, **44**(18-19):5912-5929. [doi:10.1016/j.ijsolstr.2007.02.006]

El Fatmi, R., 2007b. Non-uniform warping including the effects of torsion and shear forces. Part II: analytical and numerical applications. *International Journal of Solids and Structures*, **44**(18-19):5930-5952. [doi:10.1016/j.ijsolstr.2007.02.005]

Firouz-Abadi, R.D., Haddadpour, H., Novinzadehb, A.B., 2007. An asymptotic solution to transverse free vibrations of variable-section beams. *Journal of Sound and Vibration*, **304**(3-5):530-540. [doi:10.1016/j.jsv.2007.02.030]

Gruttmann, F., Wagner, W., 2001. Shear correction factors in Timoshenko's beam theory for arbitrary shaped cross-sections. *Computational Mechanics*, **27**(3):199-207. [doi:10.1007/s004660100239]

Gruttmann, F., Sauer, R., Wagner, W., 1999. Shear stresses in prismatic beams with arbitrary cross-sections. *International Journal for Numerical Methods in Engineering*, **45**(7):865-889. [doi:10.1002/(SICI)1097-0207(19990710)45:7<865::AID-NME609>3.0.CO;2-3]

Hutchinson, J.R., 2001. Shear coefficients for Timoshenko beam theory. *Journal of Applied Mechanics*, **68**(1):87-92. [doi:10.1115/1.1349417]

Ibrahim, S.M., Carrera, E., Petrolo, M., Zappino, E., 2012. Buckling of composite thin walled beams using refined theory. *Composite Structures*, **94**(2):563-570. [doi:10.1016/j.compstruct.2011.08.020]

Ieşan, 1986. On Saint-Venant's problem. *Archive for Rational Mechanics and Analysis*, **91**(4):363-373. [doi:10.1007/BF00282340]

Jensen, J.J., 1983. On the shear coefficient in Timoshenko's beam theory. *Journal of Sound and Vibration*, **87**(4):621-635. [doi:10.1016/0022-460X(83)90511-4]

Kaneko, T., 1975. On Timoshenko's correction for shear in vibrating beams. *Journal of Physics D: Applied Physics*, **8**(16):1927-1936. [doi:10.1088/0022-3727/8/16/003]

Kim, C., White, S.R., 1997. Thick-walled composite beam theory including 3-D elastic effects and torsional warping. *International Journal of Solids and Structures*, **34**(31-32):4237-4259. [doi:10.1016/S0020-7683(96)00072-8]

Kim, J.S., Wang, K.W., 2010. Vibration analysis of composite beams with end effects via the formal asymptotic method. *Journal of Vibration and Acoustics*, **132**(4):041003. [doi:10.1115/1.4000972]

Kosmatka, J.B., Lin, H.C., Dong, S.B., 2001. On Saint-Venant's problem for an inhomogeneous, anisotropic cylinde—part II: cross-sectional properties. *Journal of Applied Mechanics*, **68**(3):382-391. [doi:10.1115/1.1365152]

Ladevèze, O., Simmonds, J., 1996. New concepts for linear beam theory with arbitrary geometry and loading. *Proceedings of the Academy of Sciences. Series II, Mechanics, Physics, Chemistry, Astronomy*, **332**(6):445-462 (in French).

Ladevèze, O., Simmonds, J., 1998. New concepts for linear beam theory with arbitrary geometry and loading. *European Journal of Mechanics - A/Solids*, **17**(3):377-402. [doi:10.1016/S0997-7538(98)80051-X]

Ladevèze, P., Sanchez, P., Simmonds, J., 2004. Beamlike (Saint-Venant) solutions for fully anisotropic elastic tubes of arbitrary closed cross section. *International Journal of Solids and Structures*, **41**(7):1925-1944. [doi:10.1016/j.ijsolstr.2003.11.006]

Lin, H.C., Dong, S.B., 2006. On the Almansi-Michell problems for an inhomogeneous, anisotropic cylinder. *Journal of Mechanics*, **22**(1):51-57. [doi:10.1017/S1727719100000782]

Matsunaga, H., 1996. Buckling instabilities of thick elastic beams subjected to axial stresses. *Computers & Structures*, **59**(5):859-868. [doi:10.1016/0045-7949(95)00306-1]

Nali, P., Carrera, E., Lecca, S., 2011. Assessments of refined theories for buckling analysis of laminated plates. *Composite Structures*, **93**(2):456-464. [doi:10.1016/j.compstruct.2010.08.035]

Novozhilov, V.V., 1961. Theory of Elasticity. Pergamon Press, Oxford.

Popescu, B., Hodges, D.H., 2000. On asymptotically correct Timoshenko-like anisotropic beam theory. *International Journal of Solids and Structures*, **37**(3):535-558. [doi:10.1016/S0020-7683(99)00020-7]

Rand, O., 1994. Free vibration of thin-walled composite blades. *Composite Structures*, **28**(2):169-180. [doi:10.1016/0263-8223(94)90046-9]

Roberts, T.M., Al Ubaidi, H., 2001. Influence of shear deformation on restrained torsional warping of pultruded FRP bars of open cross-section. *Thin-Walled Structures*, **39**(5):395-414. [doi:10.1016/S0263-8231(01)00009-X]

Roberts, T.M., Al Ubaidi, H., 2002. Flexural and torsional properties of pultruded fiber reinforced plastic I-profiles. *Journal of Composites for Construction*, **6**(1):28-34. [doi:10.1061/(ASCE)1090-0268(2002)6:1(28)]

Saadé, K., Espion, B., Warzée, G., 2004. Non-uniform torsional behavior and stability of thin-walled elastic beams with arbitrary cross-sections. *Thin-Walled Structures*, **42**(6):857-881. [doi:10.1016/0961-9526(92)90035-5]

Samanta, A., Kumar, A., 2006. Distortional buckling in monosymmetric I-beams. *Thin-Walled Structures*, **44**(1):51-56. [doi:10.1016/j.tws.2005.09.007]

Schardt, R., 1966. Eine erweiterung der technischen biegetheorie zur berechnung prismatischer faltwerke. *Der Stahlbau*, **35**:161-171 (in German).

Schardt, R., 1994. Generalized beam theory—an adequate method for coupled stability problems. *Thin-Walled Structures*, **19**(2-4):161-180. [doi:10.1016/0263-8231(94)90027-2]

Schardt, R., Heinz, D., 1991. Structural Dynamics, Chapter Vibrations of Thin-Walled Prismatic Structures under Simultaneous Static Load Using Generalized Beam Theory. Balkema, Rotterdam, p.921-927.

Silvestre, N., 2002. Second-order generalised beam theory for arbitrary orthotropic materials. *Thin-Walled Structures*, **40**(9):791-820. [doi:10.1016/S0263-8231(02)00026-5]

Silvestre, N., 2007. Generalised beam theory to analyse the buckling behaviour of circular cylindrical shells and tubes. *Thin-Walled Structures*, **45**(2):185-198. [doi:10.1016/j.tws.2007.02.001]

Silvestre, N., Camotim, D., 2002. First-order generalised beam theory for arbitrary orthotropic materials. *Thin-Walled Structures*, **40**(9):791-820. [doi:10.1016/S0263-8231(02)00026-5]

Sokolnikoff, I.S., 1956. Mathematical Theory of Elasticity. McGraw-Hill.

Stephen, N.G., 1980. Timoshenko's shear coefficient from a beam subjected to gravity loading. *Journal of Applied Mechanics*, **47**(1):121-127. [doi:10.1115/1.3153589]

Timoshenko, S.P., Woinowski-Krieger, S., 1970. Theory of Plate and Shells. McGraw-Hill.

Tsai, S.W., 1988. Composites Design, 4th Ed. Think Composites, Dayton.

Turvey, G.J., 1996. Lateral buckling test on rectangular cross-section of pultruded GRP cantilever beams. *Composites Part B Engineering*, **27**(1):35-42. [doi:10.1016/1359-8368(95)00004-6]

Volovoi, V.V., Hodges, D.H., Berdichevsky, V.L., Sutyrin, V.G., 1999. Asymptotic theory for static behavior of elastic anisotropic I-beams. *International Journal of Solid Structures*, **36**(7):1017-1043. [doi:10.1016/S0020-7683(97)00341-7]

Wagner, W., Gruttmann, F., 2002. A displacement method for the analysis of flexural shear stresses in thin walled isotropic composite beams. *Computers & Structures*, **80**(24):1843-1851. [doi:10.1016/S0045-7949(02)00223-7]

Yu, W., Hodges, D.H., 2004. Elasticity solutions versus asymptotic sectional analysis of homogeneous, isotropic, prismatic beams. *Journal of Applied Mechanics*, **71**(1):15-23. [doi:10.1115/1.1640367]

Yu, W., Hodges, D.H., 2005. Generalized Timoshenko theory of the variational asymptotic beam sectional analysis. *Journal of the American Helicopter Society*, **50**(1):46-55. [doi:10.4050/1.3092842]

Yu, W., Volovoi, V.V., Hodges, D.H., Hong, X., 2002. Validation of the variational asymptotic beam sectional analysis (VABS). *AIAA Journal*, **40**(10):2105-2113. [doi:10.2514/2.1545]